



Proceedings of the Fifteenth International Conference on
Computational Structures Technology
Edited by: P. Iványi, J. Kruis and B.H.V. Topping
Civil-Comp Conferences, Volume 9, Paper 11.2
Civil-Comp Press, Edinburgh, United Kingdom, 2024
ISSN: 2753-3239, doi: 10.4203/ccc.9.11.2
©Civil-Comp Ltd, Edinburgh, UK, 2024

Forming Processes of a Retaining Ring based on the Response Surface Method

G. Shi

School of Mechanical and Automobile Engineering
Guangxi University of Science and Technology
Liuzhou, China

Abstract

A one-stroke forming process for retaining ring-type parts is proposed. The method is based on the traditional two-step stamping and forming process, and the mechanical analysis of the forming process of the retaining ring components is carried out to obtain a mechanical formula applicable to the indentation of retaining ring parts, and the design of the mold structure scheme is combined with the principle of the indentation process. The effects of the maximum offset of the top of the formed blank, the temperature and the top rounding angle on the thick wall of the formed part and the mold wear, respectively, were discussed using DEFORM and response surface methods, and a regression prediction model with two response variables on each of the three independent variables was obtained to optimize the optimal geometric structure parameters of the blank, which was finally verified by physical tests. Finally, a test mold was designed based on the simulation results of the formed parts to realize production processing and verify the feasibility of the one-step forming process method.

Keywords: retaining ring type parts, DEFORM, mold design, response surface method, forming process, regression forecasting model

1 Introduction

In the modern manufacturing industry, structural light weighting, low energy consumption and near-net forming of parts are the development themes in the world of manufacturing[1]. Especially in the field of automobile and its parts manufacturing,

there are many medium-thickness rotary parts, and if the traditional multi-step forming process is still used, not only the production efficiency is low, energy consumption is high, but also there are defects such as the macroscopic comprehensive mechanical properties of the parts are not high and the micro structure is not uniform, which obviously does not meet the social development requirements of modern green manufacturing and precision forming [2].

At present, most of the domestic and foreign for wheel retaining ring forming to spin forming, mold forming mostly, spinning process of more passes, forming accuracy is difficult to control, and after repeated heating will lead to grain growth, easy to produce defects, and low production efficiency, high labor intensity, more suitable for small batch production. The simple mold structure, high dimensional accuracy and forming efficiency of mold forming make it easy to realize integral forming, which not only avoids the instability of quality and size of spin forming, but also ensures the integrity of the component and the continuity of the flow line [6]. It is not difficult to find out that the die-notching is the most suitable forming process method for such components, and the existing production process is often through two or even three times forming, which cannot adapt to the production needs, therefore, whether one die-notching can become the focus of this research.

The shrink forming process is a forming process in which the initial formed pipe is reduced in diameter by means of a shrink forming die. As a more mature forming process with the advantages of simple forming, uniform deformation and few defects, it has been widely recognized by domestic and foreign scholars in the forming of mostly conical components [7]. Researchers have mainly focused on further refinement and deepening of the optimization of key process parameters such as billet volume selection, indentation force, and ultimate indentation coefficient.

]

In the theoretical study, Hu Chengwu et al. [8-9] analyzed the shrinkage force and shrinkage size by using the principal stress method and energy method under neglecting and considering the effect of wall thickness variation and work hardening, respectively, and proposed and verified a new mathematical model of shrinkage force. The Strozhev and Onkursov formulas considering wall thickness variation and work hardening were also compared and verified, and the results showed that the wall thickness variation and hardening effect had a significant effect on the indentation force. Lu Xianfeng [10-11] et al. derived the calculation of the indented part billet by geometric relations, and discussed the calculation of the key technical parameters of the indentation, and derived and verified the calculation formula of the tube billet indentation forming. Langui Xu[12] analyzed the law of indentation forming for different busbars and applied the principal stress method to derive the calculation formula of indentation force. In terms of forming process, the research in recent years has mainly focused on the research on the combination of the indentation and other processes, and the expansion of the application of the indentation process. Li et al [6] thickened an aircraft tie rod using the indentation process and conducted an in-depth

discussion on the rheological law of the material and the process parameters affecting the thickening of the tube under hot pressing to derive the deformation law of the indentation thickening.

As a more mature forming process, it has the advantages of simple forming, uniform deformation and less defects, etc. It has been widely recognized by domestic and international scholars in the forming of mostly conical members [7]. Researchers have mainly focused on further refinement and deepening of the optimization of key process parameters such as billet volume selection, indentation force, and ultimate indentation coefficient.

In the theoretical study, Hu Chengwu [8-9] et al. analyzed the shrinkage force and shrinkage size by using the principal stress method and energy method under neglecting and considering the effect of wall thickness variation and work hardening, respectively, and proposed and verified a new mathematical model of shrinkage force. The Strozhev and Onkursov formulas considering wall thickness variation and work hardening were also compared and verified, and the results showed that the wall thickness variation and hardening effect had a significant effect on the indentation force. Lu Xianfeng [10-11] et al. derived the calculation of the indented part billet by geometric relations, and discussed the calculation of the key technical parameters of the indentation, and derived and verified the calculation formula of the tube billet indentation forming. Langui Xu [12] analyzed the indentation forming laws for different busbars and applied the principal stress method to derive the calculation formula for the indentation force. In terms of forming process, the research in recent years has focused on the combination of shrinkage and other processes and the expansion of the application of shrinkage process. Li et al [6] thickened an aircraft tie rod using the indentation process and conducted an in-depth discussion on the rheological law of the material and the process parameters affecting the thickening of the tube under hot pressing to derive the deformation law of the indentation thickening. Hideki Utsunomiya and Hisashi Nishimura [13] proposed that changing the form of the bus bar in the wrinkle-prone area from a straight line to a curve during the shrinkage of thin-walled tubes could significantly reduce the wrinkling phenomenon and at the same time could reduce the shrinkage forming force. Liu, J.S. [14] et al. achieved the forming of thin-walled tubes with large wall thicknesses at smaller indentation coefficients through indentation and upsetting die design, and the process can increase the deformation of the metal by 2 to 2.5 times. With the development of computer computing power, numerical simulation presents obvious advantages in the analysis of the indentation process and gradually becomes an important tool for the selection of process design parameters. Wang Huizhong [15] carried out finite element simulation of the pipe spin-punch indentation process and realized the three-dimensional thermodynamic coupling numerical simulation and simulation of the process through the control of boundary conditions and simulation parameters. Lu Y [16] proposed an approximate theory for calculating the selection of process

parameters such as forming shape and indentation coefficient based on the volume invariance and Levy-Mises criterion, and investigated the effect of loading rate on forming in the spherical die indentation process of tubes. Chen et al. [17] analyzed the effect of different die cone angles and different friction factors on the shrinkage of titanium alloy tubes, and the analysis showed that the wall thickness of the tubes could be increased by increasing the die cone angle and the friction factor. Wu Ang et al. [18] proposed an indentation forming method applicable to large tapered parts and compared the axial indentation forces during this indentation forming with those of standard straight-walled tapered parts by the principal stress method to arrive at the best forming solution.

Based on the above-mentioned literature, the forming mechanism and process of forming tapered parts with indentation are predominant in die compression forming, and the research methods tend to be mature, and they all focus on tapered parts with small indentation coefficients or tubular aluminum parts with large indentation coefficients. Therefore, it is the focus of this paper to propose a new method for the production process of such parts, to study the forming process and the form of the mold, and to fully verify the feasibility of the scheme through experiments.

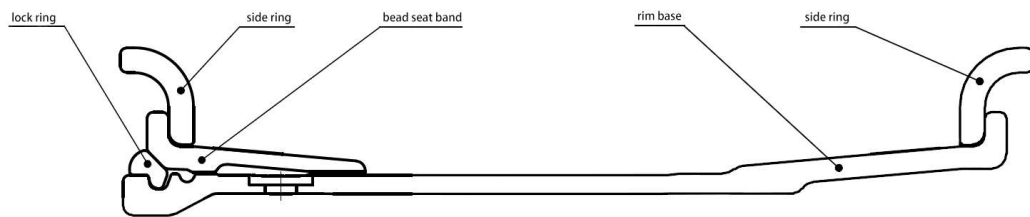


Fig. 1: Schematic diagram of five-piece rim structure

2 Forming Process Development

2.1. Process Analysis

The retaining ring part drawing is shown in the figure, the outer diameter of the part is 1447.6mm, the height is 78mm and the thickness is 20mm. The existing retaining ring forming process is a rolled cylinder, flaring (shrinkage), and forming process. Based on the existing production process, it is envisioned that whether the pre-forming stage can be skipped to achieve a single shrinkage forming is worth further study (Fig. 2).

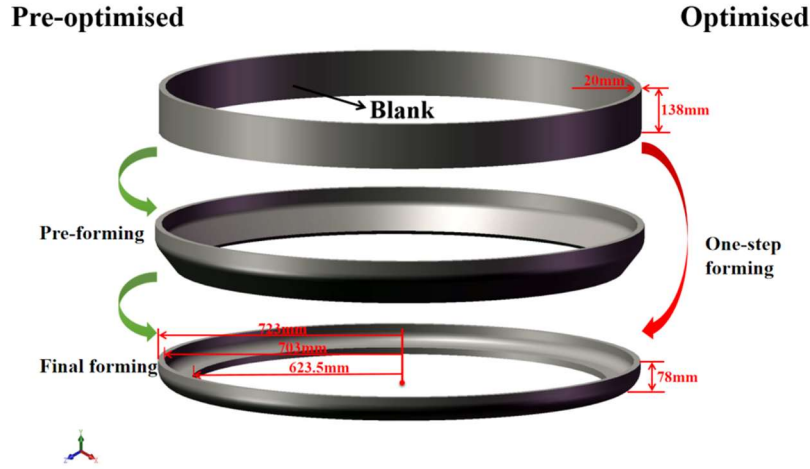


Fig. 2: Diagram of retaining ring forming process before and after optimization

The indentation forming theory is the basis of the indentation forming test, and an accurate theoretical analysis can make an effective judgment for the subsequent development of the plan. The degree of indentation deformation is measured by the indentation factor m_s , whose corresponding expression is

$$m_s = \frac{d}{D} \quad (1)$$

In the formula (1): d is the diameter after the shrinkage process; D is the diameter before the shrinkage process. The degree of shrinkage deformation is generally expressed by the limit shrinkage coefficient m_{smin} , which is constrained by the instability condition, and its value is mainly related to the mechanical properties of the material, billet size, mold structure, etc. The smaller the limit shrinkage coefficient of the elastic-plastic material, the greater the degree of shrinkage deformation is often allowed. In general, the ultimate indentation coefficient of elastoplastic soft steel is taken as 0.70-0.80[11]. The calculated indentation coefficient of the retaining ring studied in this paper is: 0.82. The number of indentations n is calculated as

$$n = \frac{\lg \frac{s}{m_{sp}}}{\lg m_{sp}} \quad (2)$$

In the formula (2), m_s is the indentation coefficient, m_{sp} is the average indentation coefficient, take $m_{sp} \approx m_{smin} = 0.70$, the calculated $n = 0.6 < 1$, so theoretically we can get the part can be molded in one sequence.

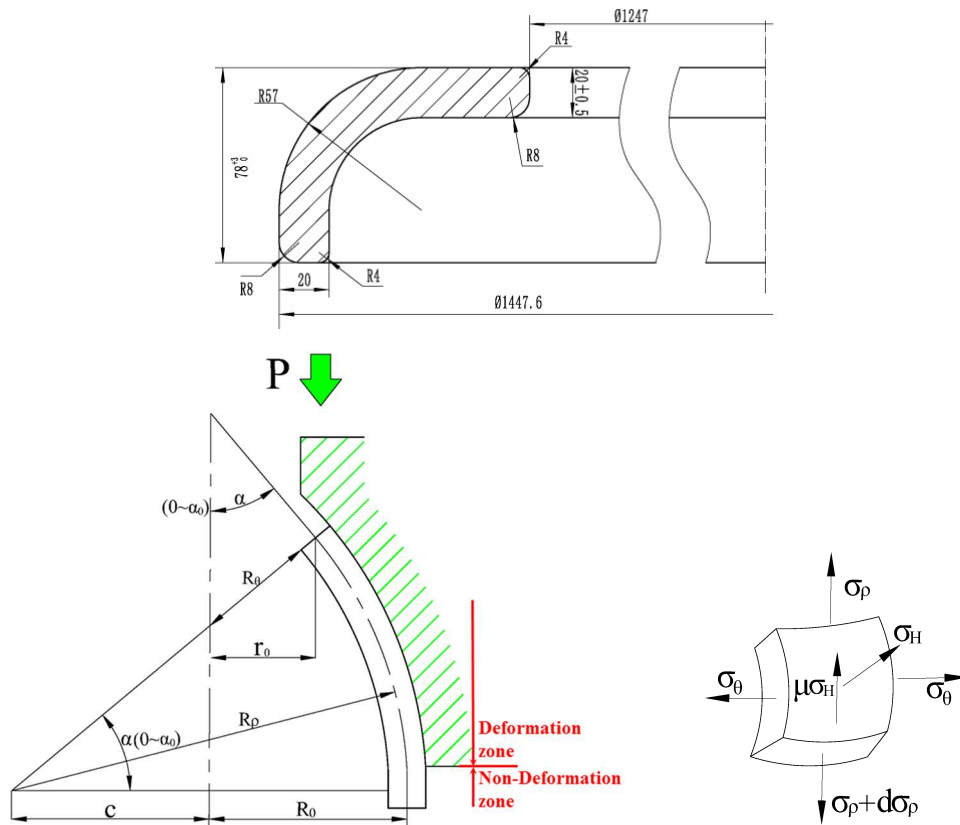
2.2. Mechanical Analysis

In the existing theoretical analysis of the indentation force, the stress analysis about the indentation forming tapered parts is more perfect, and Lu [10] et al. in the consideration of variable wall thickness indentation notch die as a linear model of the indentation force method tends to be matured.

$$P = 1.15K\pi R_0 s_0 (1 + \mu \cot \alpha) \cos \alpha \left[\left(1 + \frac{n}{2}\right) (1 - m - Inm) + n(1 - m)(2m^2 - 7m - 31)/12 \right] \quad (3)$$

In the formula (3), n and K are the material constants at a certain temperature, m is the shrinkage factor, R_0 is the barrel radius, S_0 is the wall thickness, and α is the half cone angle.

However, it can be concluded from the diagram of the retaining ring parts in Fig.3 that the analysis of its dimensional characteristics, if the use of indentation notch die for linear form fear cannot meet the requirements. Therefore, it is necessary to consider the forming of parts with varying wall thickness and curved busbar, for which Wu Ang and Gao Chang [18,19] et al. analyzed mechanically the forming process of rotary tapered parts and proposed a mechanical model of indentation. Considering the effect of thickness variation, the thickness variation assumption is introduced, i.e., the final thickness of the billet after forming is linearly related to the radius. The wall thickness is constantly changing and tends to increase, which also provides a theoretical basis for the subsequent optimization of the billet parameters.



(a) Geometric analysis of notch die shrinkage forming (b) Stress state diagram of unit body in deformation area

Fig. 4: Force analysis of blank indentation forming

Since the indentation deformation belongs to axisymmetric deformation, the equilibrium equation can be obtained according to the film theory of axisymmetric rotary shell [20] and the stress state diagram of the unit body in the indentation deformation zone shown in Fig. 4 (a).

$$\rho \frac{d\sigma_\rho}{d\rho} + \sigma_\rho \left(1 + \frac{\rho ds}{s d\rho}\right) - \sigma_\theta - \frac{\mu\rho}{\sin\alpha} \left(\frac{\sigma_\rho}{R_\rho} + \frac{\sigma_\theta}{R_\theta}\right) = 0 \quad (4)$$

Where: s is the thickness of the material after deformation; μ is the coefficient of friction; σ_ρ is the axial stress; σ_θ is the circumferential stress.

Fig. 4(b) shows the deformation geometry analysis, dividing the blank into two regions: deformation zone and non-deformation zone. By analyzing the change process of the blank during the indentation process of the circular indentation notch die in Fig. 4(b), the following three geometric relationships can be derived.

$$\rho = R_\rho \cos \alpha - c \quad (5)$$

$$d\rho = -R_\rho \sin \alpha \quad (6)$$

$$R_\theta = R_\rho - \frac{c}{\cos \alpha} \quad (7)$$

For thin-walled indentation forming with larger R_ρ , the strain state in the deformation zone can be approximated as planar, due to the stable indentation deformation process, the deformation zone enters the plastic state, which is obtained according to the criterion of Quresga [21].

$$\sigma_\theta = -\beta\sigma_s \quad (8)$$

where: β is the coefficient, generally takes 1-1.155, in this paper $\beta = 1$; σ_s is the yield stress.

Substituting the geometric relations (5) to (7) into equation (4), we can calculate:

$$\sigma_\rho = \frac{1-\mu\alpha}{\cos\alpha - /R_\rho} \{C + \sigma_s [2\mu \sin \alpha - (1 + \mu\alpha) \cos \alpha]\} \quad (9)$$

Substituting the boundary conditions, when $\alpha = \alpha_0$, the stress $\alpha_\rho = 0$, we can find the constant C:

$$C = -\sigma_s [2\mu \sin \alpha_0 (1 + \mu\alpha_0) \cos \alpha_0] \quad (10)$$

Therefore, the stress σ_ρ along the axial direction can be expressed as:

$$\sigma_\rho = -\frac{\sigma_s(1-\mu\alpha)}{\cos\alpha - c/R_\rho} [(1+\mu\alpha)\cos\alpha - (1+\mu\alpha_0)\cos\alpha_0 + 2\mu(\sin\alpha_0 - \sin\alpha)] \quad (11)$$

The effect of the change in the thickness of the blank on the σ_ρ acting on the wall of the blank during the shrinkage process is analyzed. According to the stress-strain increment theory [21] there is:

$$d\varepsilon_{ij} = \sigma_{ij}d\lambda \quad (12)$$

Where: ε_{ij} is the strain component; σ_{ij} is the stress component; λ is the instantaneous non-negative scaling factor.

For the plane stress state, the velocity relationship between stress and strain can be expressed as $\dot{\varepsilon}_\rho, \dot{\varepsilon}_\theta, \dot{\varepsilon}_t$ which denote the radial, tangential and normal phase variation rates, respectively.

$$\frac{\sigma_\theta - \sigma_\rho}{\sigma_\theta} = \frac{\dot{\varepsilon}_\rho - \dot{\varepsilon}_\theta}{\dot{\varepsilon}_\theta - \dot{\varepsilon}_t} \quad (13)$$

According to the principle of constant volume and substitution into equation $\dot{\varepsilon}_\rho = \dot{\varepsilon}_\theta + \dot{\varepsilon}_t$ yields.

$$\frac{\sigma_\rho}{\sigma_\theta} = \frac{2\dot{\varepsilon}_t + \dot{\varepsilon}_\theta}{\dot{\varepsilon}_t - \dot{\varepsilon}_\theta} \quad (14)$$

For the deformation zone part, the stress σ_ρ is a function of α . According to the plastic strain condition Eq. (8), the values of σ_θ and σ_ρ are substituted into the stress-strain rate Eq. (14) to obtain.

$$\dot{\varepsilon}_t = -\frac{1+k}{2-k}\dot{\varepsilon}_\theta \quad (15)$$

From equation (15), it can be seen that $\dot{\varepsilon}_t$ and $\dot{\varepsilon}_\theta$ are directly opposite to each other, indicating that the thickness of the billet in the deformation area gradually increases during the indentation forming process, when the strain rate is converted into strain, the final thickness of the blank cylinder wall in the deformation area can be calculated using the above formula.

$$\varepsilon_t = \ln \frac{s}{s_0} \quad (16)$$

$$\varepsilon_\theta = \ln \frac{\rho}{R_0} \quad (17)$$

The expressions for the final wall thickness can be derived by combining (15) to (17).

$$s = s_0 \left(\frac{R_0}{\rho} \right)^{\frac{1+k}{2-k}} \quad (18)$$

Substituting equation (18) in (11) by associating (5) to (7), it is known that when $\alpha = \alpha_0$, the stress $\sigma_\rho = 0$. As the angle α decreases, α_0 increases, and at $\alpha = 0$, the instantaneous yield stress applied to the billet reaches a maximum value $\sigma_{\rho 1}$. The equation can be derived.

$$\sigma_{\rho 1} = -\frac{\sigma_s}{1-c} [1 - (1 + \mu \alpha_0) \cos \alpha_0 + 2\mu \sin \alpha_0] \quad (19)$$

From the equation can be obtained, in the initial stage of the indentation, the material yielding occurs, at this moment the axial direction of the concave die downward pressure. And when $\alpha = \pi/2$, the indentation deformation is terminated and the forming of the part is completed, at this time the formed part is subjected to the maximum stress $\sigma_{\rho 2}$ in the axial direction, the expression is.

$$\sigma_{\rho 2} = \frac{\sigma_s (1 - \mu \pi / 2)}{c / R_\rho} [(1 + \mu \alpha_0) \cos \alpha_0 + 2\mu (\sin \alpha_0 - 1)] \quad (20)$$

where σ_ρ is the transformation relation for α_0 , thus introducing the common relation for trigonometric functions.

$$\cos \alpha_0 = \frac{c+r_0}{R_\rho}, \sin \alpha_0 = \frac{\sqrt{R_\rho^2 - (c+r_0)^2}}{R_\rho}, \alpha_0 = \arccos \frac{c+r_0}{R_\rho}$$

Substituting into equation (19) yields:

$$\sigma_{\rho 1} = -\sigma_s \left[1 - \frac{r_0}{R_0} + 2\mu \frac{\sqrt{R_\rho^2 - (r_0 - R_\rho - R_0)^2}}{R_0} - \mu \frac{r_0 - R_\rho - R_0}{R_0} \arccos \frac{r_0 - R_\rho - R_0}{R_0} \right] \quad (21)$$

Combining the above trigonometric relations $\frac{c}{R_\rho} = \frac{R_\rho - R_0}{R_\rho}$ for R_0, R_ρ, r_0 , we get

$$\sigma_{\rho 1} = -\sigma_s \left[1 - \frac{r_0}{R_0} + \frac{\mu}{R_0} \sqrt{R_\rho^2 - (r_0 - R_\rho - R_0)^2} \right] \quad (22)$$

The formula (22) is the maximum axial stress in the deformation region of the billet during the shrinkage deformation, so the expression of the shrinkage force during the shrinkage deformation is derived:

$$P = 2\pi R_0 s_0 \sigma_{\rho 1} \quad (23)$$

2.3. Mold Design Solutions

As mentioned above in the literature, Xu Langui and Wu Ang [12,18] have compared the mechanical models of indentation with curved and straight indentation die bases for the same degree of indentation coefficient and indentation deformation, and pointed out that the indentation force when the die bases are curved is much smaller than the magnitude of the indentation force when they are straight, thus reducing the risk of instability of the blank during the forming process to a certain extent.

Based on the above research, the concave and convex die structure is designed based on the dimensional characteristics of the retaining ring parts, as shown in Fig5. In the ideal case, when the billet is subjected to circumferential load after the radial compression rather than diameter reduction, the billet in the constraints of the die cavity to get the idealized part structure, but in the actual production test, with the downward movement of the upper die, the top deformation zone of the billet material yielded to the occurrence of shrinkage deformation. The non-deformed area at the bottom of the blank is slightly deformed by the load, and the stress is shown in Fig6, which leads to radial instability at the bottom of the blank and causes defects in the forming quality of the part. In response to the above problem, an annular retaining ring structure (Fig.6) is designed on the outside of the convex die to form a radial limit while effectively preventing the part from destabilizing during the indentation process, thus effectively avoiding this defect.

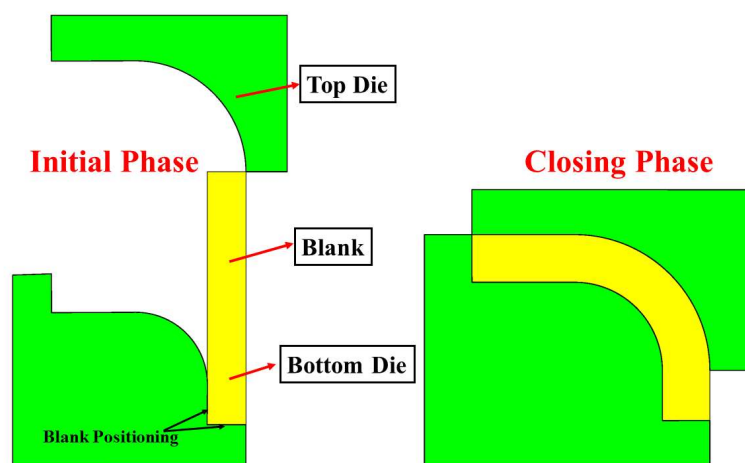


Fig. 5: Mold scheme development

3 Determination of the influence factors and building the finite element model

3.1. Determination of the factors influencing the blanks

Common small size parts in the shrink forming process because of its small shrink force, short stroke, the blank is usually in the form of equal wall thickness. And for the medium-thick cylinder large indentation coefficient of shrink forming, the wall thickness of the deformation zone is larger, the degree of shrink deformation and the more deformed material, the greater the axial stress and radial compression stress during shrinkage. If you want to reduce the radial compressive stress of the billet and also to ensure the dimensional requirements of the part, the billet deformation area can be designed as a variable wall thickness in accordance with the stress-strain thickening theory to reduce the degree of material deformation, reduce the shrinkage force and improve the forming quality. On the basis of the original equal wall thickness billet, the intersection of deformation and non-deformation area is taken as the reference, the top offset angle is noted as β and the maximum offset is noted as α . Therefore, the variable wall thickness dimension, i.e. the maximum offset, is taken as the primary influencing factor for the forming quality of the billet.

Accordingly, during the initial forming stage, the billet is loaded directly by the inner wall of the concave die to the top of the billet, causing it to yield to deformation. Therefore, the design of a proper rounded structure on the top of the blank, noted as R, can increase the contact area with the inner wall of the die and therefore effectively reduce the degree of wear of the die. Secondly, based on Zhang Ya's study of tube shrink forming, it is shown that the warm and hot forming processes contribute to less tube ultimate shrinkage coefficient under linear temperature field conditions, thus improving the forming quality. In addition, combined with the existing production process of retaining ring means, it is not difficult to find that warm forming can obtain a hot high material strength and ductility, so the initial temperature of the blank before shrinkage is recorded as an important influencing factor affecting its forming quality. In summary, the range of values between the factors affecting the forming of blanks is determined (Table 1).

<i>Factor</i>	<i>Name</i>	<i>Units</i>	<i>Type</i>	<i>Minimum</i>	<i>Maximum</i>
A	λ (Top offset)	mm	Numeric	0.5	2
B	T(Temperature)	°C	Numeric	500	800
C	R(Top chamfer)	mm	Numeric	0	4

Table 1: Value of each factor of the billet

To develop the response factors for the experimental program, the thickness S of the formed part was used as the primary response variable in the test plan, based on

the principle of equal volume, in conjunction with the requirements for the use of the part. In order to reduce the wear of the die and prolong the life of the die during indentation forming, it is also important to control the surface wear of the die, so the wear of the inner wall of the die is recorded as W as another response variable.

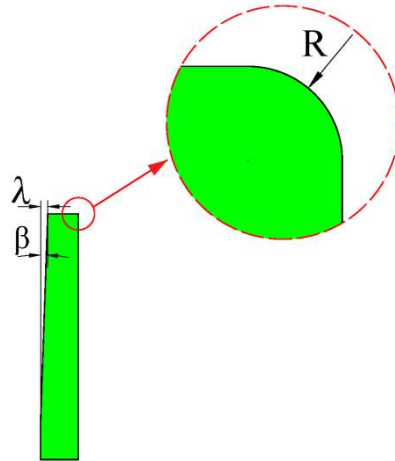


Fig.7. Initial structural parameters of the blank

3.2. Finite element modeling

CREO software is used to build the blank, concave die and convex die models respectively, and determine the relative positions and assembly relationships between the components according to the simulation requirements, forming a complete assembly as shown in Figure 8, and importing them into DEFORM respectively. The blank is set as a plastic body, the material is selected as 1035, the die is a rigid body, the pressing speed of the concave die is 1mm/s, the friction coefficient between the die and the blank is 0.25, and the thermal conductivity is 11N/sec/mm/C. In order to better observe the stress and strain states during the molding process, two-dimensional cross-sections are used for simulation.

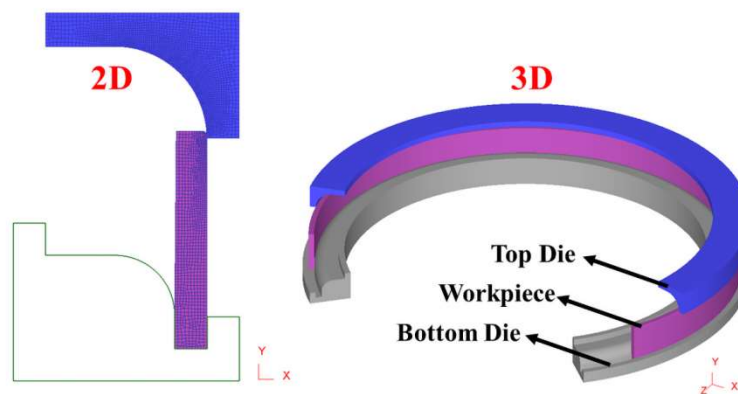


Fig. 8: Finite element model

4 Response surface method to optimize billet parameters

4.1. Box-Behnken test design and results

The results of the experimental scheme and calculations by Box-Behnken design are shown in Table 2.

Std	Run	Factrol B:T (°C)	Factrol C:R (mm)	Responsel Max Thickness (mm)	Response2 Wear(mm)
1	13	750	2	20.21	8.50E-05
2	16	750	2	20.15	8.13E-05
3	4	850	2	20.26	7.23E-05
4	8	850	2	20.1	6.93E-05
5	2	800	0	20.23	0.00056
6	17	800	0	20.09	0.00061
7	5	800	4	20.24	7.13E-05
8	3	800	4	20.06	6.60E-05
9	11	750	0	20.12	0.00045
10	6	850	0	20.2	8.20E-05
11	10	750	4	20.16	7.40E-05
12	15	850	4	20.22	2.31E-05
13	12	800	2	20.13	9.00E-05
14	7	800	2	20.12	8.95E-05
15	1	800	2	20.14	7.84E-05
16	9	800	2	20.1	6.70E-05
17	14	800	2	20.09	8.50E-05

Table 2: Box-Behnken experimental design

4.2. Response surface modeling and results analysis

In the finite element simulation of part forming, the relationship between process parameters and measures of forming quality is highly complex, nonlinear, and cannot be expressed in expressions. Therefore, a response surface model is needed to represent the relationship between the two instead of the original model. The mathematical expression of the polynomial response surface method is

$$y = \beta_0 + \sum_{i=1}^k \beta_i x_i + \sum_{i=1}^k \beta_{ii} x_i^2 + \sum_{i=1}^{k-1} \sum_{j=i+1}^k \beta_{ij} x_i x_j + \zeta \quad (21)$$

where: y is the dependent variable; x_i and x_j are design variables; $i=1,2,3,\dots,k$; $j=i+1$; k is the number of design variables; $\beta_0, \beta_i, \beta_{ij}$, is the response surface regression coefficient; and ζ is the fitting error.

Design-Expert 8.0.6 software was used to set the fitting term to the quadratic model to obtain the best fit results, and the ANOVA of the response surface quadratic equation was used to analyze the variance. Table 3,4 shows that the fitted multivariate nonlinear model of part thickness and die wear on the three factors passed the F-test

to obtain a significance probability p-value less than 0.0500, and the misfit term 3.49 was greater than 0.1000, indicating that the test results and the mathematical model fit well.

From the results of ANOVA in Table 3, it can be seen that the probability of significance of the three factors: A offset < B temperature < C chamfer, indicating that in the response surface model of part forming thickness, the magnitude of influence on the results of wall thickness dimensions is in the order of: offset, temperature, and chamfer. From the results of ANOVA in Table 4, it can be seen that the probability of significance of the three factors: C chamfer < B temperature < A offset, indicating that in the response surface model of concave die wear, the magnitude of influence on the results of wear is in the order of: chamfer, temperature, and offset. Among them, the p-values of significance probability for both offset and chamfer are much less than 0.05, which indicates a greater influence on the results of the response surface model.

<i>Source</i>	<i>Squares</i>	<i>df</i>	<i>Square</i>	<i>Value</i>	<i>Prob > F</i>
Model	0.054	9	5.977E-003	6.73	0.0100
<i>A</i>	0.036	1	0.036	41.02	0.0004
<i>B</i>	2.450E-003	1	2.450E-003	2.76	0.1408
<i>C</i>	2.000E-004	1	2.000E-004	0.23	0.6496
<i>AB</i>	2.500E-003	1	2.500E-003	2.81	0.1374
<i>AC</i>	4.000E-004	1	4.000E-004	0.45	0.5238
<i>BC</i>	1.000E-004	1	1.000E-004	0.11	0.7471
<i>A</i> ²	2.038E-003	1	2.038E-003	2.29	0.1737
<i>B</i> ²	7.427E-003	1	7.427E-003	8.36	0.0233
<i>C</i> ²	1.217E-003	1	1.217E-003	1.37	0.2802
Residual	6.220E-003	7	8.886E-004		
<i>Lack of Fit</i>	4.500E-003	3	1.500E-003	3.49	0.1294

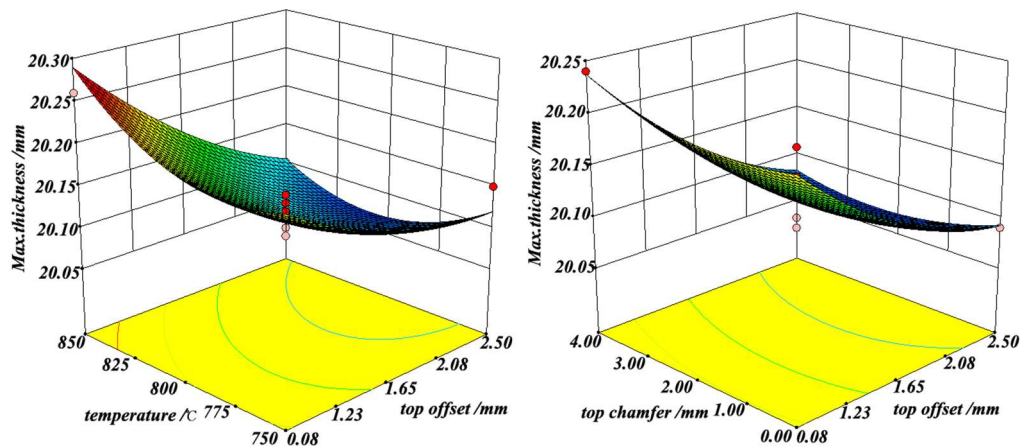
Table 3: Thickness response surface model ANOVA

<i>Source</i>	<i>Squares</i>	<i>df</i>	<i>Square</i>	<i>Value</i>	<i>Prob > F</i>
Model	4.890E-007	9	5.434E-008	5.87	0.0146
<i>A</i>	1.805E-010	1	1.805E-010	0.020	0.8929
<i>B</i>	2.460E-008	1	2.460E-008	2.66	0.1471
<i>C</i>	2.692E-007	1	2.692E-007	29.09	0.0010
<i>AB</i>	1.225E-013	1	1.225E-013	1.323E-005	0.9972
<i>AC</i>	7.645E-010	1	7.645E-010	0.083	0.7821
<i>BC</i>	2.514E-008	1	2.514E-008	2.72	0.1433
<i>A</i> ²	2.850E-008	1	2.850E-008	3.08	0.1227
<i>B</i> ²	3.207E-008	1	3.207E-008	3.47	0.1050
<i>C</i> ²	1.113E-007	1	1.113E-007	12.02	0.0104
Residual	6.479E-008	7	9.256E-009		
<i>Lack of Fit</i>	6.443E-008	3	2.148E-008	233.93	< 0.0001

Table 4: Thickness response surface model ANOVA

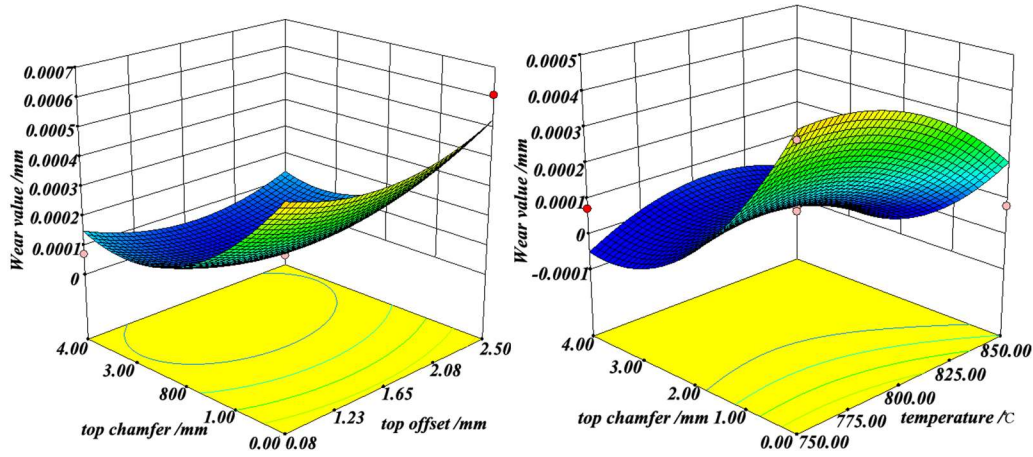
From the Fig 9 can be obtained: the most important factor affecting the maximum tolerance thickness value after the final forming of the part is the value of the billet variable wall thickness size, followed by the temperature, with the increase of the billet variable wall thickness size, that is, the increase of the value of the top offset, the maximum thickness value has a significant tendency to reduce. Correspondingly, when the temperature increases, as the strength of the material decreases, the fluidity increases, and the higher the temperature will likewise lead to an increase in the thickness tolerance value. In particular, the variation in thickness tolerance values caused by the forming process of this part is due to the gap between the upper and lower dies or the error in the closed area of the die, which is an uncontrollable and unavoidable factor.

From Fig. 10 it can be obtained that the factor affecting the change of the wear value of the concave die during the forming process of the part is mainly the size of the top rounded corner, followed by the temperature. On the one hand, it can be seen from (a) that as the value of the top rounding increases, the size of the wear of the concave die tends to decrease gradually, while in the process of pressing down the concave die, the stiffness of the blank in the axial direction changes due to the presence of the top offset, and the material is easily deformed, which also has an impact on the value of the wear of the concave die. On the other hand, it can be seen from (b) that as the value of top rounding increases and the temperature of the blank increases, the wear of the concave die reaches its optimum.



(a) Maximum thickness versus top offset and temperature (b) Maximum thickness versus top offset and temperature

Fig. 9: Three factors on the maximum thickness response surface



(a) Relationship between wear value on top offset and rounding (b) Relationship between wear value on top rounding and temperature.

Fig.10: Response surface of three factors on wear value

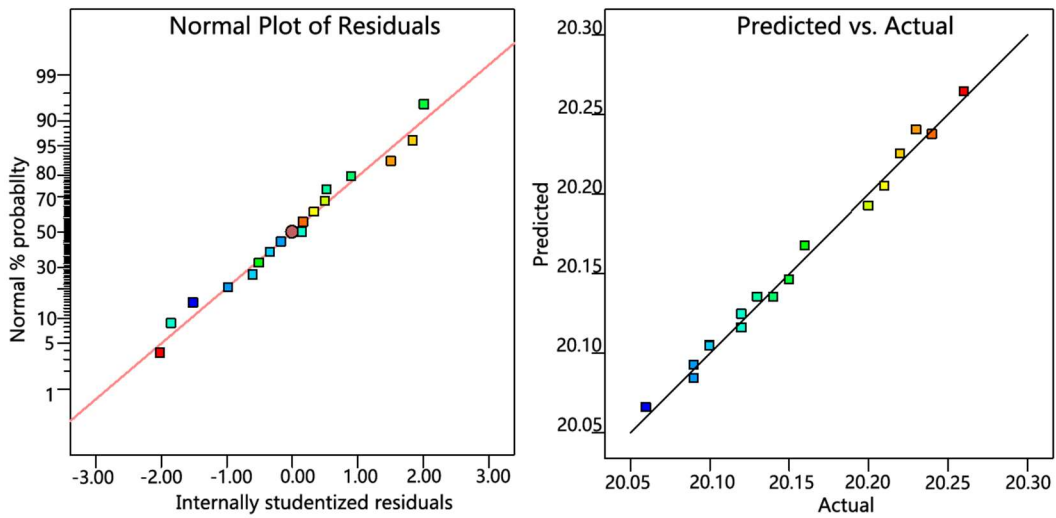
Figure 11 shows the correspondence between the predicted values of the model and the experimental values. The linearity of the distribution of the data is obvious, and there are no abnormal data points. All points in Figs. 11a and 11b are basically linearly distributed, indicating that the two prediction models on indentation force and height can effectively explain the variation relationship of the three factors with high accuracy.

4.3. Determination of optimal dimensional parameters

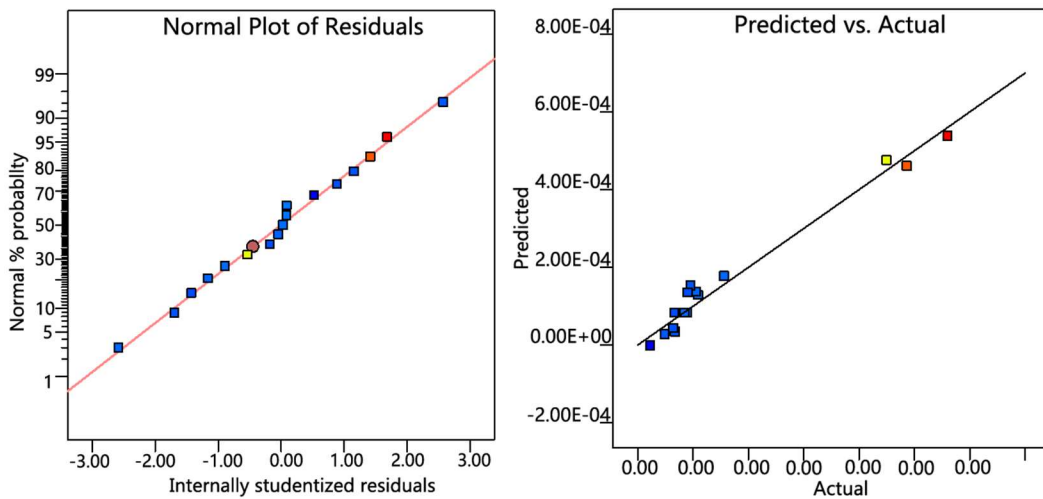
After eliminating the factors with significance probability greater than 0.05 by response surface analysis of Box-Behnken experimental design, the final multiple nonlinear regression equations of thickness and die wear with respect to (A) top offset λ , (B) temperature T , and (C) top chamfer R can be derived. The regression model is as follows.

$$\begin{aligned}
 H &= +20.12 - 0.068A + 0.017B + 5.000E - 003C - 0.025AB - 1.000E \\
 &\quad - 002AC - 5.000E - 003BC + 0.022A^2 + 0.042B^2 + 0.017C^2 \\
 P &= +8.198E - 005 + 4.750 - 006A - 5.545E - 005B - 1.835E - 004C \\
 &\quad + 1.750E - 007AB - 1.382E - 005AC + 7.927E - 005BC \\
 &\quad + 8.227E - 005A^2 - 8.728E - 005B^2 + 1.626E - 004C^2
 \end{aligned}$$

In the actual production test, in order to meet the dimensional requirements of the product, it is necessary to make the thickness tolerance of the billet after forming as small as possible, and the mold wear value is minimized. The optimal geometric parameters of the blank are obtained by setting the range of the three factors and the extreme values of the two response variables through the automatic optimization function of Design-expert software: $\lambda=2.39\text{mm}$, $T=824.82^\circ\text{C}$, $R=2.81\text{mm}$.



(a) Thickness



(b) Wear value

Fig.11: Data point distribution map.

5 Load Travel Variation

The optimal parameters of the blank obtained after optimization by response surface method are simulated. The stroke-load curve obtained from the simulation with the optimal parameters is shown in Figure 12. The maximum forming load value at this time is 6003 tons, and it can be seen from the simulation results that the forming quality is better and can meet the forming requirements when forming under the optimal parameters.

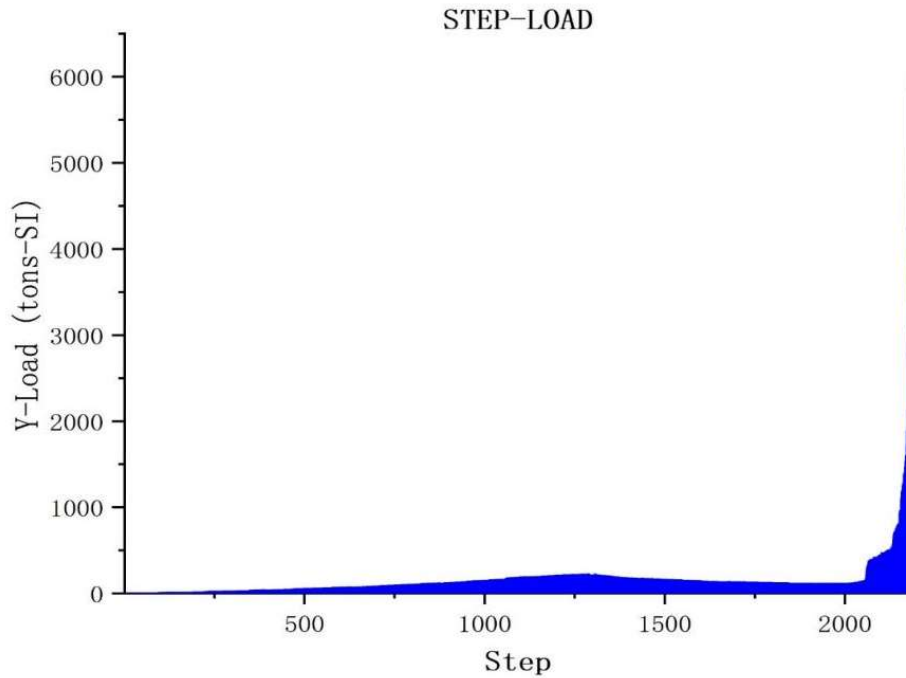


Fig. 12: Curve of stroke-forming load under optimal parameters

6 Equivalent Force-Strain Analysis

In the process of shrinkage deformation of the blank, the stress distribution on the billet is shown in Figure 13 with a gradual increase of the equivalent force. At the initial stage of shrinkage, the top of the billet part is in contact with the concave die. As the deformation intensifies, the area to be deformed enters the bending deformation process, the material at the inner bend of the billet is extruded, the stress change in the non-deformed area is not obvious, and the stress in the deformed area gradually increases. After the end of forming, the maximum equivalent stress area is mainly distributed in the deformation area and non-deformation area on both sides, which is due to the huge load on the part in the final forming stage, so that the stress concentration distribution at both ends of the part. The maximum equivalent force value is 286 MPa.

Similarly, the strain distribution on the blank during the forming process of the part shows a gradual increase as shown in Figure 14. The maximum value of the strain zone is mainly distributed in the flange area of the contact of the convex die and the transition area between the rounded corner of the concave die and the side wall, and the inner and outer ends of the bending section of the indentation deformation zone are deformed, and with the depth of the bending deformation these areas are deformed more. The maximum equivalent effect variation value is 0.429 mm.

7 Experimental Verification

According to the results of the one-step forming process scheme obtained from the simulation, the test tool was designed and the stamping test was carried out. 16000kN four-column hydraulic press was selected, Q123B was selected as the test material, and the cylinder blank was selected, and the ambient temperature was room temperature (26°C). The results are shown in Fig15. The formed parts are free of defects such as folding, instability and rebound, and can meet the requirements of the design drawings, which are basically consistent with the simulation results, proving the accuracy of the finite element simulation and verifying the feasibility of one-time stamping and forming of flange-type parts.

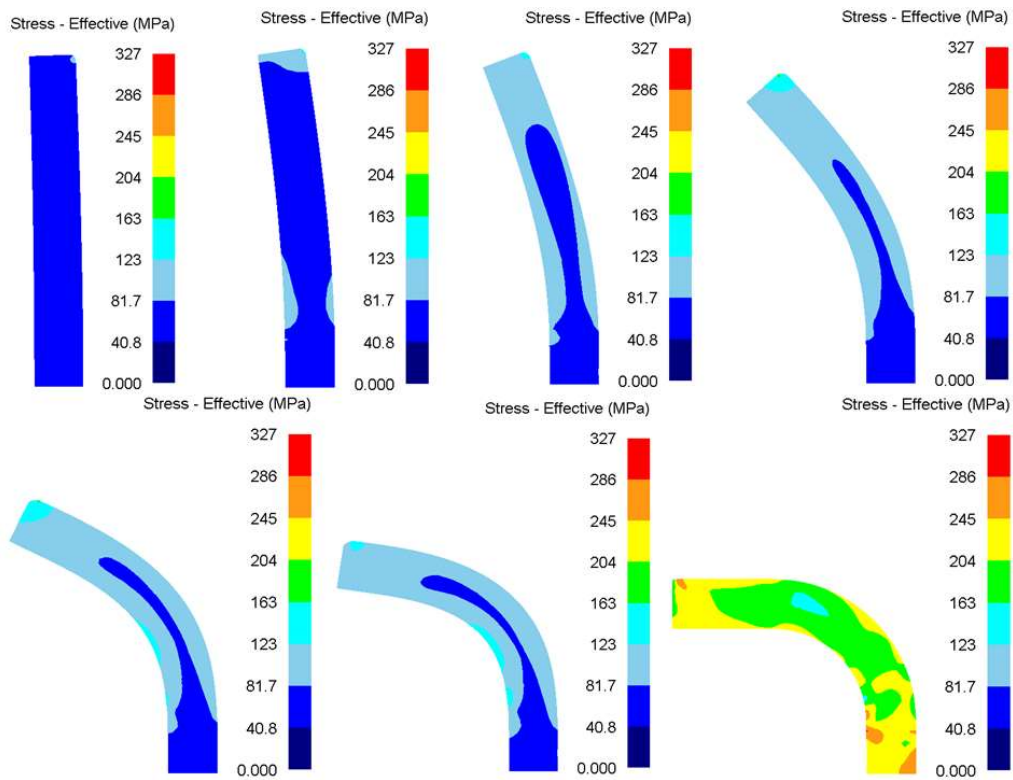


Fig.13. Equivalent stress distribution

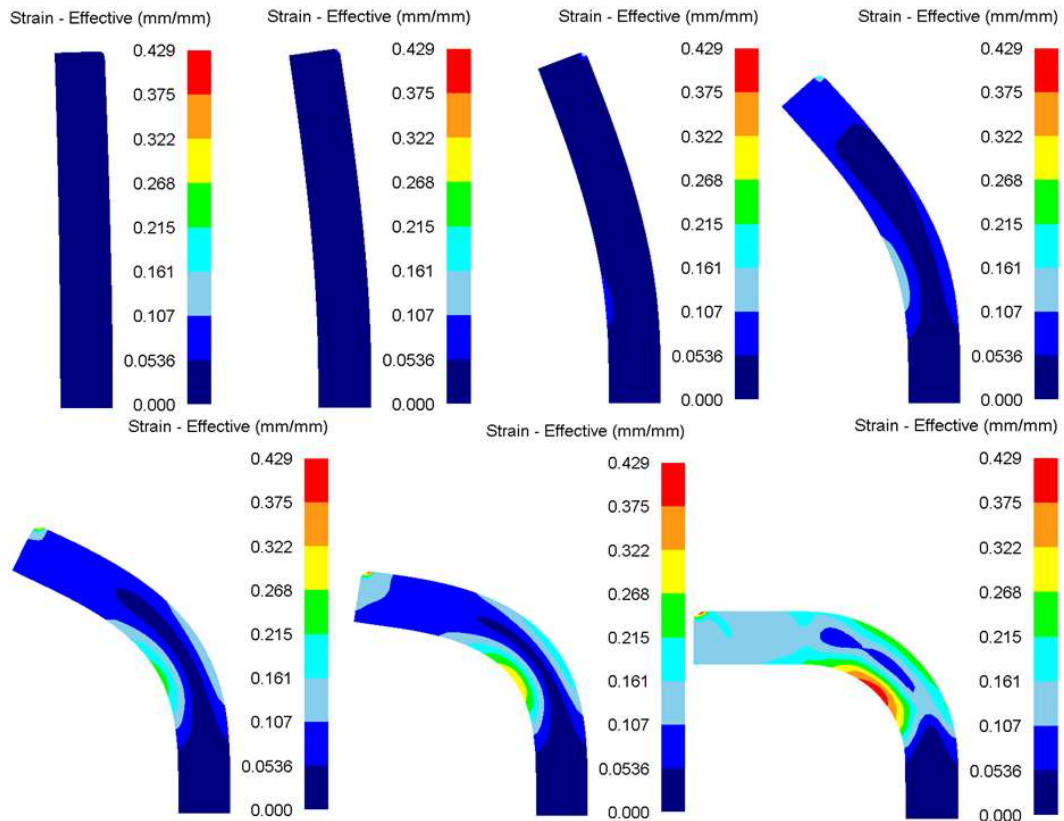


Fig.14. Equivalent strain distribution



(a) Physical drawing of the formed part (b) Four-column hydraulic press
Fig. 1.: Forming test

8 Conclusion

(1) This paper proposes an indentation forming process method for retaining ring-type parts, and calculates to determine the theoretical feasibility of the one-sequence scheme according to the principle of indentation. And the mechanical analysis of the forming process was carried out to obtain an expression for the indentation forming force of retaining ring type parts. A mold structure design scheme was developed to obtain a mold structure design method applicable to the molding of such parts.

(2) A multivariate nonlinear regression model of part thickness and mold wear is fitted by the response surface method to calculate the optimal geometric parameters of the blank structure that result in small part thickness tolerance and mold wear. $\lambda=2.39\text{mm}$, $T=824.82^\circ\text{C}$, $R=2.81\text{mm}$. And the test verification was carried out, and the results showed that the errors were all less than 10%, which fully verified the ideal degree of the mathematical model for calculating the indentation force. This demonstrates the feasibility of the simulation test and the reliability of the mathematical model.

References

- [1] Zhen Qian, Yong Sun, Yaguang Li, Chang Wang, Paul A. Meehan, William J.T. Daniel, Shichao Ding, Investigation of the design process for the Chain-die forming technology based on the developed multi-stand numerical model, *Journal of Materials Processing Technology*, Volume 277, 2020, 116484, ISSN 0924-0136.
- [2] Xiao-hui Shen, Wei Chen, Jun Yan, Lei Zhang, Jing Zhang, Experiment and Simulation of Metal Flow in Multi-stage Forming Process of Railway Wheel. *Journal of Iron and Steel Research, International*, Volume 22, Issue 1, 2015, Pages 21-29, ISSN 1006-706X.
- [3] Wang Tao. Finite element analysis and optimization design of heavy-duty cargo vehicle frame[D]. Dalian Jiaotong University, 2020.
- [4] Fang, G, Gao, WR. & Zhang, XG. Finite element simulation and experiment verification of rolling forming for the truck wheel rim. *Int. J. Precis. Eng. Manuf.* 16, 1509–1515, 2015.
- [5] Kang W.J, Kim K.A, Kim G.H., Fatigue failure prediction of press fitted parts subjected to a cyclic loading condition by finite element methods, *Fatigue & Fracture of Engineering Materials & Structures*, 2007, 30(12): 1194-1202.
- [6] LI Xuanying, Research on rheological behavior of thin-walled aluminum alloy tube necking and thickening on hot extrusion, Nanchang : Nanchang Hangkong University, 2017.
- [7] Almeida B.P.P, Alves M.L., Rosa P.A.R., et al. Expansion and reduction of thin-walled tubes using a die: Experimental and theoretical investigation, *International Journal of Machine Tools & Manufacture*, 2006, 46(12–13):1643-1652.
- [8] Hu C.W., Luo W.B., Peng Y.R., Theoretical calculation and experimental verification of the indentation force of conical concave die, *China Engineering Science*. 2005(06): 54-56.
- [9] Hu C.W., Luo W.B., Peng Y.R., Comparison of methods for calculating indentation stresses in conical notches, *Forging and pressing technology*, 2005(03): 63-65.
- [10] Lu X.F., Tao Y.Q., Meng F.S., On the calculation model of curved type indented part blanks, *Journal of Nanchang University (Engineering Edition)*. 2013(01): 49-53.

- [11] Lu X.F., Pan J.Z., Yang A. Calculation formula for conical type indented parts blanks[J]. Precision forming engineering. 2012(06): 99-102.
- [12] Xu Langui, Ruan Feng, Li Zhendong. Study on neck bending of thin-walled cylindrical parts with straight pipes with indentation deformation, Forging and pressing technology. 2010(01): 32-35.
- [13] Hideki Utsunomiya, Hisashi Nishimura, Development of die necking technique for thinner wall of DI can, Journal of the Japan Plastics Processing Society, 1998, 39: 60-64 .
- [14] Liu Junsheng, Zhang Caili, Zheng Qiming, Liu Xiaocui, Design and forming process of composite die for partial heating shrinkage and upsetting of pipe parts, Forging and pressing technology, 2006(04):57-58.
- [15] Wang Huizhong, Numerical simulation and modeling of spin indentation forming of copper tubes, University of Electronic Science and Technology, 2011.
- [16] Lu Y., Study of preform and loading rate in the tube nosing process by spherical die, Computer Methods in Applied Mechanics and Engineering, 2005, 194(25–26): 2839-2858.
- [17] Chen C.Y., Chen T.C., Experimental and numerical analysis of titanium alloy microtube tube-end nosing forming, Materials Science Forum, 2018, 16-21.
- [18] WU Ang, WU Ying, LI Guojun, LI Xubin, Zhang Zhimin, Design and multi-geometry parameter optimization of indentation forming process for large tapered parts based on response surface method[J]. Journal of Mechanical Engineering, 2019, 55(24):83-92.
- [19] Jia Li-li, Ke Xu-gui, Gao Jin-zhang, Shen Li-qin, Kang Zhi-jun, Stamping Process and Die Design, Posts and Telecommunications Press, 201608.330.
- [20] Zhang Ya, Study on deformation rule and thickness thickening of tube necking process under non-uniform temperature field, Beijing Mechanical Science Research Institute, 2015.
- [21] Wang D.N., Principle of Metal Plastic Forming, Beijing: China Machine Press, 1995.
- [22] Wang Songlin, Zhang Xing, Li Guojun, Liu Cuixia, Finite element research on shrinkage forming process of bowl parts, Forging & stamping equipment & manufacturing technology, 2015, 50 (02): 92-95.